EPJ Web of Conferences **140**, 15002 (2017) DOI: 10.1051/epjconf/201714015002
Powders & Grains 2017

Comparison between a μFE model and DEM for an assembly of spheres under triaxial compression

Sadegh Nadimi[1,*], *Tom* Shire[2], and *Joana* Fonseca[1]

[1]City, University of London, London, UK
[2]Imperial College London, London, UK

Abstract. This paper presents a simple case of a Face Centred Cubic (FCC) array of 2,000 spheres under triaxial compression to compare the results obtained using the Discrete Element Method (DEM) and a micro finite element model (μFE). This μFE approach was developed so that the internal structure of the soil can be obtained using x-ray computed tomography and converted into a numerical fabric. The individual grains are represented as continuum deformable bodies and the inter-granular interaction based on the defined contact laws. In order to demonstrate the simple contact constitutive behaviour used in this μFE model, the response for two contacting elastic spheres is compared with theoretical equations. The strength at failure of the packing of 2,000 spheres is seen to yield similar values for DEM, μFE and the analytical solution. When comparing the evolving void ratio, a good agreement between the two numerical models was observed for very small strains but as the strain increases, the values start to diverge, which is believed to be related with the rigidity of the grains used in DEM.

1 Introduction

The mechanical behaviour of granular materials is originated from the transmission of forces between the grain to grain contacts [1]. The use of discrete numerical modelling approaches enables the measurement of grain-scale forces and stresses, which it is not a trivial task in experiments. In particular, Discrete Element Method (DEM) has been widely used for the modelling of grain interactions within the assembly, assuming purely elastic and for the most part, spherical grains [2, 3]. The importance of particle shape in force transmission has been highlighted in a number of studies *e.g.* [4, 5] and several attempts have been made to include particle shape in DEM approaches, *e.g.* [6, 7]. Regarding the contact constitutive behaviour, the Hertz [8] and Mindlin & Deresiewicz [9] models, were developed to model two spheres in contact, a case for which the contact evolves from a point to a circle under normal loading. These contact models are therefore of limited application to represent contact interaction of non-spherical grains. Another difficulty in DEM simulations is representing the initial packing (void ratio) of a granular assembly from experiments [10]. An irregular packing of spheres can be prepared using gravity with high computational cost.

A two dimensional microstructure-based finite element (μFE) model, which employ the natural depositional grain scale characteristics of a sand has been proposed by Nadimi *et al.* [11]. The initial packing, grain shape and grain sizes are captured using images obtained from micro Computed Tomography (μCT). The contact behaviour between two irregular grains comes from stress propagation and concentration within the body of the grains and is unique for different contact topology and grain morphology [12]. To consider full contact interaction of irregular grains, the extension of μFE model to three-dimensions (3D) is under development by the authors.

In this paper, the proposed methodology is firstly reviewed. Then, the principles are verified against theoretical solutions. Finally, the response of an assembly of spheres under triaxial loading is compared with DEM simulations.

2 The μFE model

The principle of this μFE model is that the physical phenomena of the deformation of real soil can be investigated using a detailed numerical representation of the constituent grains (obtained from μCT) to simulate grain interaction. Thus, an accurate and tractable representation of the complex geometries of real grains can be acquired and used to enhance our understanding of force and stress transmission between grains. A summary of the methodology for generating a μFE model is shown in Fig. 1. In this Section, each part of methodology is explained in short.

* Corresponding author: sadegh.nadimi-shahraki@city.ac.uk

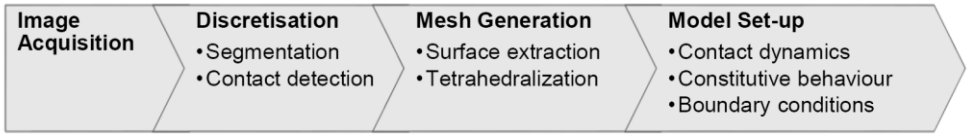

Fig. 1. Flow chart showing the steps involved in the proposed 3D μFE model

2.1 Image acquisition & discretisation

The first step is image acquisition. By using x-ray micro-computed tomography, the internal structure of the soil is obtained including shape, size and fabric [13]. The images are maps of x-ray attenuation based on the density and atomic composition of the material represented by the intensity of each voxel.
In order to obtain the individual grains, the step termed here of discretisation, two steps are involved. Firstly, the solid phase has to be extracted from the void space. A thresholding technique was employed for this part. Successively, the touching grains have to be separated to obtain the individual grains by using a morphological watershed approach [14].

2.2 Mesh generation

The numerical approximation of the problem starts from mesh generation in the μFE framework. A key requirement is to obtain an accurate representation of the object boundary. An advanced surface reconstruction algorithm was employed to extract the grain surface. Triangular iso-surfaces with an adjustable density are extracted from the 3D segmented image. The surface extraction technique employed is a refinement of the constrained Delaunay tetrahedralisation [15]. The second stage is the filling of grain with the tetrahedral elements for the sub-volumes bounded by the iso-surfaces to obtain the volumetric mesh. A MATLAB script has been developed to generate the image-based mesh. Fig. 2 shows an example of two silica sand grains with different features meshed for numerical simulation.

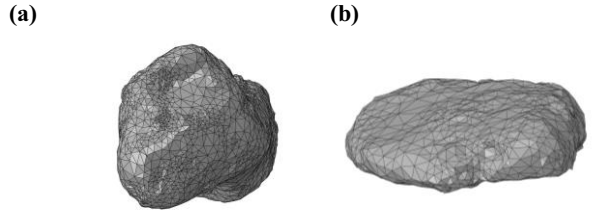

Fig. 2. An example of generated mesh from μCT images of two silica sand grains.

2.3 Model set-up

The generated mesh is imported into the finite-discrete numerical domain [16]. The model is implemented in Abaqus explicit, which uses a dynamic framework [17].
The contacts properties are defined as '*hard contact'* in the normal direction and '*Coulomb friction*' in the tangential direction. Hard contact means that all the force is transmitted when two bodies are in contact. The ability of the grains to deform enables the use of a hard contact in the normal direction, *i.e*. there is no need to use a predefined contact law in this direction. For the case of pure elastic spheres, this assumption is examined in the next section to represent theoretical contact constitutive behaviour *i.e.* Hertz [8] in normal direction, Mindlin & Deresiewicz [9] in tangential direction, Lubkin [18] for torsion, Johnson [19] for rotation.

There is need to define constitutive behaviour of solid part of each grain. This can be as simple as defining elastic modulus and Poisson's ratio or incorporating fracture energy and the breakage potential of each grain. The continuum representation of each individual grain rather than the rigid assumption (used in DEM) enables the measurement of stress propagation and concentration within the grain body.

2.4 Contact interaction

The mechanical interaction between two contacting bodies includes normal loading in combination with tangential, torsional and rotational loading. The three latter loadings are the result of friction and applied normal load. The comparison between theoretical solution and numerical modelling in the framework of the μFE was conducted to verify the contact interaction assumptions. It can be seen from Fig. 3 that the μFE numerical model framework can represent the contact laws with a high precision level by only considering hard contact and Coulomb friction.

3 Triaxial test

An assembly of 2000 spherical grains with a diameter of 2.2 mm was simulated under triaxial conditions (Fig. 4). The face-centred-cubic (FCC) packing of the assembly modelled consists of 10×10 rows of spheres in the XY-plane and 20 rows in Z-direction. Rigid wall boundaries were used. The response was investigated under standard triaxial conditions. Two steps were defined for loading, 1) isotropic compression at 50kPa and 2) shearing under controlled strain. This problem was chosen due to the available theoretical solution, as presented in [20].

3.1 DEM model

The problem was modelled in the commercial DEM code PFC^{3D} [21]. The material properties used are listed in Table 1. Fig. 5 shows the response of the assembly in terms of major principal stress (σ_1) and coordination number (Z) versus axial strain (ε_a).

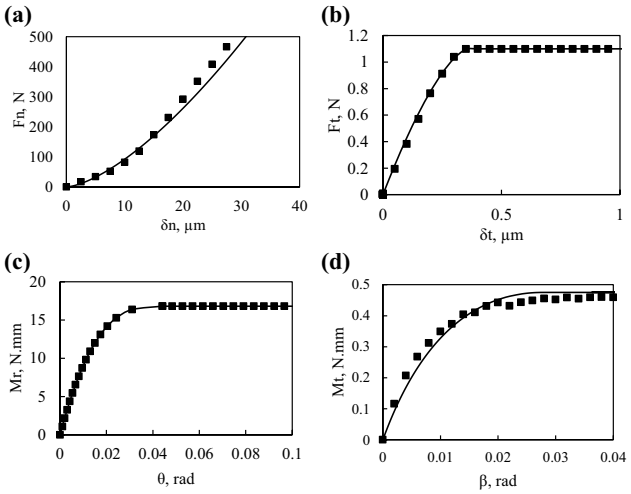

Fig. 3. Comparison between numerical simulation (square marks) and theories (solid lines) for (a) normal load: displacement, (b) tangential load: displacement, (c) rotational moment: angular displacement, and (d) torsional moment: angular displacement.

The strength at so called 'failure' is related to interparticle friction and is σ_1 = 147.6kPa for this arrangement with rigid walls. It can be seen from Fig. 5 that the failure is linked with a drop in coordination number. According to the theoretical solution [20], σ_1 is calculated from the following equation for an infinite number of grains:

$$\frac{2\sigma_1}{\sigma_2+\sigma_3}=\frac{2(1+\mu)}{(1-\mu)} \quad (1)$$

For the confining stress $\sigma_2=\sigma_3$=50kPa and interparticle friction of μ=0.22, σ_1 is equal 156.4kPa. The slightly lower value obtained from DEM can be related to the packing not being a true FCC close to the rigid boundary and the finite number of grains.

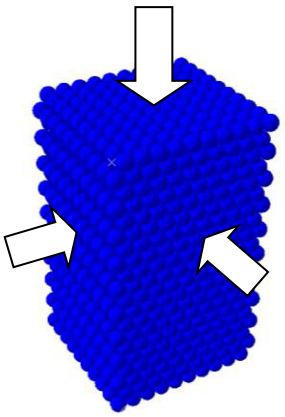

Fig. 4. 3D view of a FCC packed triaxial sample of 2,000 spheres

3.2 μFE model

The FCC model was replicated in the framework of μFE. The so called 'failure' was seen to occur at σ_1 =162.5kPa. As can be seen in Fig 3.a and also noted by [22], the Hertz theory is accurate for small normal deformation. The slight increase in the value of σ_1 can be related to normal force:displacement of deformable spheres which show higher load value than Hertz. Fig. 6a shows a deformed sphere in the μFE framework and this deformation was scaled by a factor of 50 in order to improve visualisation in Fig. 6b.

Regarding void ratio, a good agreement can be seen between DEM and μFE data (Fig. 7). It is expected to see more discrepancy in void ratio for high stress (and strain) level due to rigidity assumption in DEM simulation and DEM void ratio does discount the overlapped volume from the total solid volume.

Table 1. Material properties used for DEM and μFE simulation

Particle density	ρ	2.5 tonne/m^3
Poisson Ratio	υ	0.22 (-)
Shear modulus	G	25.82 GPa
Interparticle friction	μ	0.22 (-)
Young's modulus	E	63 GPa

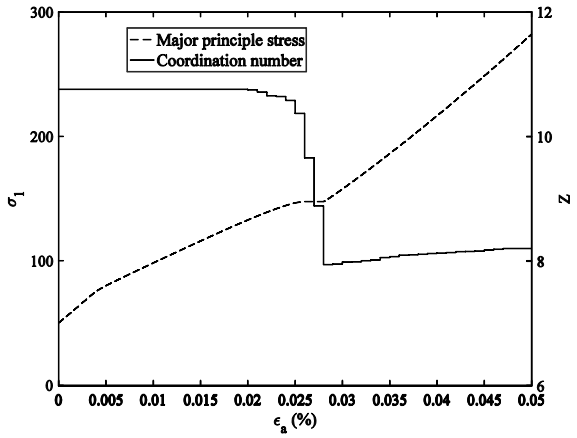

Fig. 5. Major principle stress and coordination number versus axial strain for assembly of spheres under triaxial condition obtained from DEM simulation.

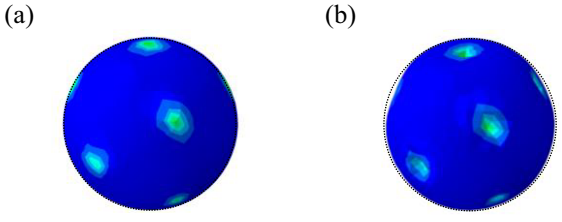

Fig. 6. Stress distribution in a deformed sphere with Z=12; deformation scale factor a) 1 and b) 50.

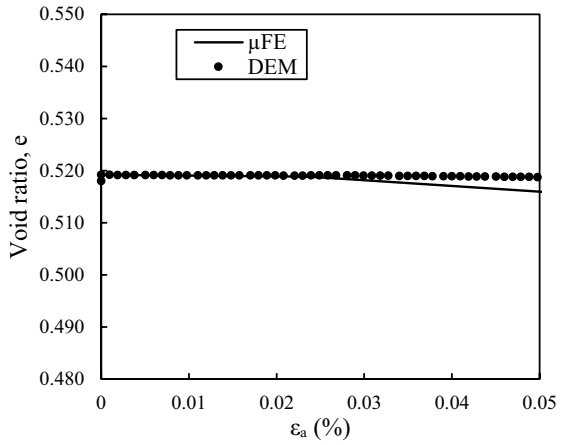

Fig. 7. Comparison of evolving void ratio between DEM and μFE models.

4 Closing remarks

A review on the development and verification of a novel μFE model was presented here. While one of the key features of the μFE model is its ability to include the morphology and fabric of real soil from μCT images, the example presented here uses spheres to simplify the comparison with DEM and analytical solutions.

An important aspect of grain scale modelling is the definition of contact laws. Despite DEM has been used for irregular shapes, it is not possible to predefine contact laws for each irregular contact topology found in natural soil. In the μFE framework, the contact behaviour comes from deformation and stress propagation within the grain, which suggests this as a robust platform to present unique contact response of grains with irregular morphology and contact topology.

It was demonstrated here that the contact constitutive behaviour used for the μFE model for an idealised elastic sphere was precisely matched with theory. The ability of this μFE approach to model large number of grains was shown and the results were seen to compare well with both DEM and the analytical solution. The divergence in the evolving void ratio when compared with the DEM results can be attributed to the deformation of the grains in the μFE model against the rigid grains used in DEM.

The μFE model described here, although computationally expensive, can provide a valuable contribution to unravel fundamental aspects of granular materials behaviour.

The first author would like to express thanks to City, University of London for his doctoral scholarship.

References

1. J. Fonseca, S. Nadimi, C.C. Reyes-Aldasoro, C. O'Sullivan, M.R. Coop, Soils & Foundations **56**, No. 5, pp. (2016).
2. C. O'Sullivan, *Particulate Discrete Element Modelling: A Geomechanics Perspective*. Spon Press (2011).
3. C. Thornton, *Granular Dynamics, Contact Mechanics and Particle System simulations*, Springer (2015).
4. I. Cavarretta, M. Coop, C. O'Sullivan, Géotechnique **60**, pp. 413–423 (2010).
5. F. N. Altuhafi, M. R. Coop, V. N. Georgiannou, J. Geotech. Geoenvironmental Eng., vol. 4016071, (2016).
6. J. Ferellec, G.R. McDowell, Géotechnique **60**, No. 3, pp. 227–232 (2010) [doi: 10.1680/geot.9.T.015].
7. G. T. Houlsby. Computers & Geotechnics, **36**, pp. 953–959, (2009).
8. H. Hertz, Journal für die reine und angewandte Mathematik, **92** (1882).
9. R.D. Mindlin, H. Deresiewiez, Elastic spheres in contact under varying oblique forces, ASME J. Appl. Mech. 20, pp. 327-344 (1953).
10. J. O'Donovan, S. Hamlin, G. Marketos, C. O'Sullivan, E. Ibraim, M. Lings, D. Muir Wood. In Geomechanics from micro to macro (eds K. Soga, K. Kumar, G. Biscontin and M. Kuo). London, UK: Taylor & Francis Group (2015).
11. S. Nadimi, J. Fonseca, R.N. Taylor, In *Deformation characteristics of geomaterials*: Proceedings of the 6th International symposium on deformation characteristics of geomaterials, Buenos Aires, Argentina (2015).
12. J. Fonseca, S. Nadimi, C.C. Reyes-Aldasoro, C. O'Sullivan, M.R. Coop, Soils & Foundations 56 (5): 818-834.
13. J. Fonseca, C. O'Sullivan, M.R. Coop, P.D. Lee, Géotechnique 63, No. 6, (2013).
14. J. Fonseca, C. O'Sullivan, M.R. Coop, AIP Conf. Proc. 1145, 223 (2009).
15. J.R. Shewchuk, Computational Geometry: Theory and Applications, 47, No. 7, pp. 741-778 (2014).
16. A. Munjiza, *The Combined Finite-Discrete Element Method,* Wiley, London (2004).
17. ABAQUS User's Manual 2016, Dassault Systèmes, version 6.14.
18. J. L. Lubkin, ASME J. Appl. Mech., Vol. **73**, pp. 183-187 (1951).
19. K.L. Johnson *Contact mechanics*. Cambridge University Press, Cambridge (1985).
20. C. Thornton, Géotechnique, 29 No. 4, pp. 441-459. (1979).
21. Itasca Consulting Group, Inc. *PFC3D-Particle Flow Code in 3 Dimensions*, ver. 5. Minneapolis: Itasca (2015).
22. Q. J. Zheng, H.P. Zhu, A.B. Yu, Powder Technology 226, pp. 130-142, (2012).